

Synthesis of Quaternary Chalcogenide Nanocrystals: Stannite $\text{Cu}_2\text{Zn}_x\text{Sn}_y\text{Se}_{1+x+2y}$

Alexey Shavel,[†] Jordi Arbiol,[‡] and Andreu Cabot^{*,†,§}

Departament d'Electrònica, Universitat de Barcelona, Barcelona 08028, Spain, Institutio Catalana de Recerca i Estudis Avançats (ICREA) and Institut de Ciència de Materials de Barcelona, CSIC, 08193 Bellaterra, CAT, Spain, and Catalonia Energy Research Institute (IREC), Barcelona 08019, Spain

Received November 9, 2009; E-mail: acabot@ub.edu

Copper-based quaternary chalcogenides have recently attracted a great deal of attention as low-cost alternatives to conventional photovoltaic materials. Among them, $\text{Cu}_2\text{ZnSnS}_4$ has been recently prepared by three different wet organometallic routes.^{1–3} In spite of this excellent progress, shape and size control of quaternary nanocrystals is still a challenge to overcome. An alternative quaternary chalcogenide with high potential for photovoltaics is $\text{Cu}_2\text{ZnSnSe}_4$ (CZTSe). CZTSe combines many advantageous characteristics for optoelectronic applications, such as a suitable band gap (1.0–1.5 eV),⁴ a high optical absorption coefficient (up to 10^5 cm^{-1}),⁵ low toxicity, and a relative abundance of its elements. In addition, CZTSe films have promising thermoelectric properties, with ZT values of ~ 0.4 at 700 K.⁶ While CZTSe films have been prepared by coevaporation,⁵ sputtering,⁷ and pulsed laser deposition,⁸ to the best of our knowledge, no report devoted to the preparation of CZTSe nanocrystals by wet chemical methods has been published to date. Here we present a colloidal synthetic route for the production of nonstoichiometric CZTSe ($\text{Cu}_2\text{Zn}_x\text{Sn}_y\text{Se}_{1+x+2y}$) nanoparticles with a narrow size distribution.

CZTSe nanoparticles were prepared by reacting amine complexes of the metal chlorides with a saturated (2.24 M; 1 mmol total) solution of selenium in trioctylphosphine (TOPSe). The metal complexes were prepared by heating metal salts with hexadecylamine (HDA) at 150 °C. In a typical preparation, 0.50 mmol of CuCl , 0.25 mmol of ZnCl_2 , 3 mmol of HDA, and 10 g of octadecene were placed in a four-neck flask and heated to 150 °C under an argon flow until a yellowish transparent solution was obtained. At this point, the solution was maintained at 150 °C for an additional 1 h to ensure removal of water and oxygen. Next, the solution was cooled to 100 °C, and 0.25 mL of a 1 M solution of SnCl_4 in heptane was injected through a septum. The tin precursor forms a white precipitate that upon heating dissolves rapidly in the reaction mixture, giving a clear solution. The mixture containing the metal complexes was then heated to 295 °C. At this temperature, 0.45 mL of TOPSe was injected into the solution. The reaction mixture was maintained at high temperature for 5 min to allow the nanoparticles to grow. Finally, the flask was rapidly cooled to room temperature. At 60 °C, 10–15 mL of solvent (chloroform or toluene) was added to the reaction mixture to prevent its solidification. The cooled solution was cleaned several times by precipitation with 2-propanol and redispersion in pure solvent.

Figure 1 shows a transmission electron microscopy (TEM) image of the CZTSe nanoparticles obtained after 5 min of reaction at 295 °C. The prepared nanoparticles are fairly monodisperse and appear to be highly faceted with polyhedral geometries. A histogram of the size distribution of a typical sample is shown in the inset of

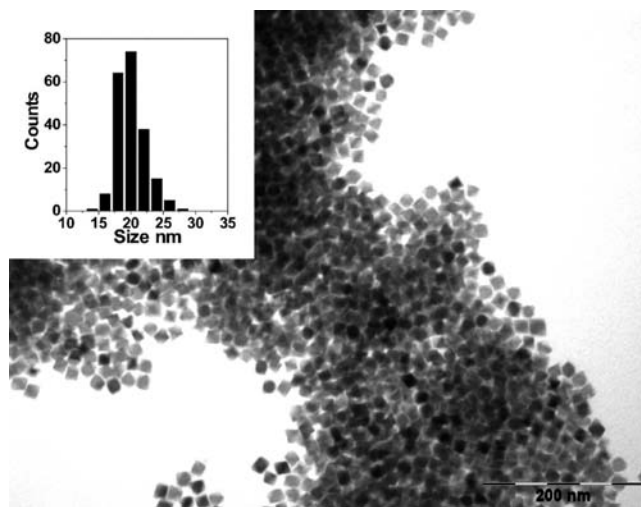


Figure 1. TEM micrograph of CZTSe nanoparticles after 5 min of reaction at 295 °C. Inset: size distribution of the prepared nanocrystals.

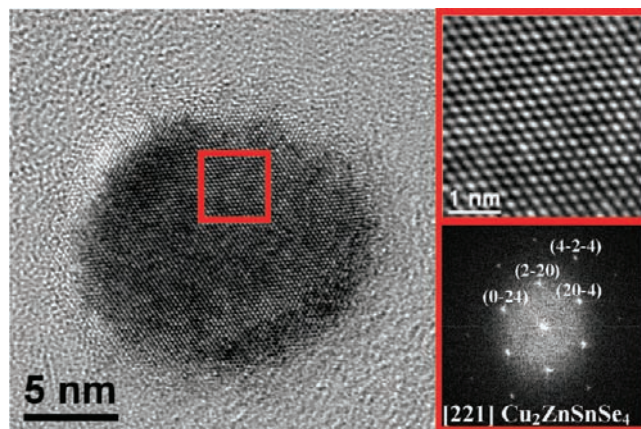


Figure 2. HRTEM micrograph of a CZTSe nanocrystal (left) with the fast Fourier transform pattern (bottom right) of the selected area of the same particle (top right).

Figure 1. The nanoparticles have an average size of 20.0 nm and a standard deviation of 2.0 nm. These values are consistent with the average size of the crystallographic domains calculated by fitting the X-ray diffraction (XRD) spectra using the Scherrer equation (23 nm).

High-resolution TEM (HRTEM) analysis of the nanoparticles (Figure 2) showed them to be single-crystalline. After power spectrum analysis, we found that the nanoparticles' crystallographic structure is compatible with the $\text{Cu}_2\text{ZnSnSe}_4$ tetragonal phase.⁹ XRD characterization of the particles' crystallographic structure (Figure

[†] Universitat de Barcelona.

[‡] Institut de Ciència de Materials de Barcelona, CSIC.

[§] Catalonia Energy Research Institute.

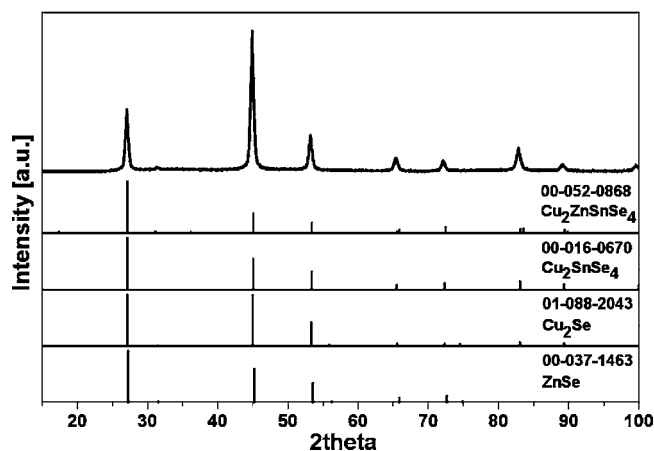


Figure 3. XRD pattern of the prepared nanoparticles. For reference, the XRD patterns of $\text{Cu}_2\text{ZnSnSe}_4$ (JCPDS 00-052-0868), Cu_2SnSe_4 (JCPDS 00-016-0670), Cu_2Se (JCPDS 01-088-2043), and ZnSe (JCPDS 00-037-1463) are also shown.

3) confirmed it to be compatible with that of CZTSe (00-052-0868; tetragonal $I\bar{4}2m$). CZTSe has a stannite-type crystal structure (space group $I\bar{4}2m$) with two tetrahedral structural units: $[\text{Cu}_2\text{Se}]$ and $[\text{SnZnSe}_4]$.⁶ The structure can be derived from zinc blende ZnSe by substitution of zinc with Cu and Sn atoms.^{10,11} Unfortunately, XRD did not allow us to make a clear distinction between CZTSe and other possible chalcogenides, such as Cu_2SnSe_4 (cubic; $F\bar{4}3m$), Cu_2Se (cubic; $Fm\bar{3}m$; synthetic berzelianite), or ZnSe (cubic; $F\bar{4}3m$; synthetic stellite). All of these structures have very close XRD patterns, as shown in Figure 3.

In order to clarify the sample composition and verify that all four elements were present in each individual nanocrystal, chemical analysis with nanoscale spatial resolution was performed. Figure 4 displays electron energy loss spectroscopy (EELS) image maps showing the elemental composition of the individual nanoparticles. This analysis shows a homogeneous distribution of the four elements Cu, Sn, Zn, and Se on the 2D-projected chemical maps of the nanocrystals. Extended EELS imaging confirmed the homogeneous composition of the sample, discarding the existence of particles with different compositions. Moreover, TEM and Z-contrast scanning TEM (STEM) micrographs showed no evidence for a nonhomogeneous composition inside each nanocrystal. Energy dispersive X-ray (EDX) analysis in combination with X-ray photoelectron spectroscopy (XPS) showed that $\sim 3\%$ of the initial Zn and $\sim 30\%$ of the Sn is accommodated inside the $\text{Cu}_2\text{Zn}_x\text{Sn}_y\text{Se}_{1+x+2y}$ stannite structure.

In conclusion, a synthetic route for the preparation of nonstoichiometric quaternary CZTSe nanoparticles has been presented. Nearly monodisperse CZTSe nanocrystals were obtained through reaction of metal amino complexes with saturated TOPSe at high temperature. The prepared nanocrystals have the tetragonal $\text{Cu}_2\text{ZnSnSe}_4$ crystallographic structure, as shown by HRTEM and XRD analyses. Nanoscale-resolved EELS spectrum images showed the presence of the four elements in each individual nanocrystal. However, quantitative analysis of the chemical composition showed the particles to be consistently Zn- and Sn-poor. Extended TEM and Z-contrast STEM analyses pointed toward a homogeneous composition in each individual nanocrystal. Further work on truly and precisely tuning the material composition is being carried out.

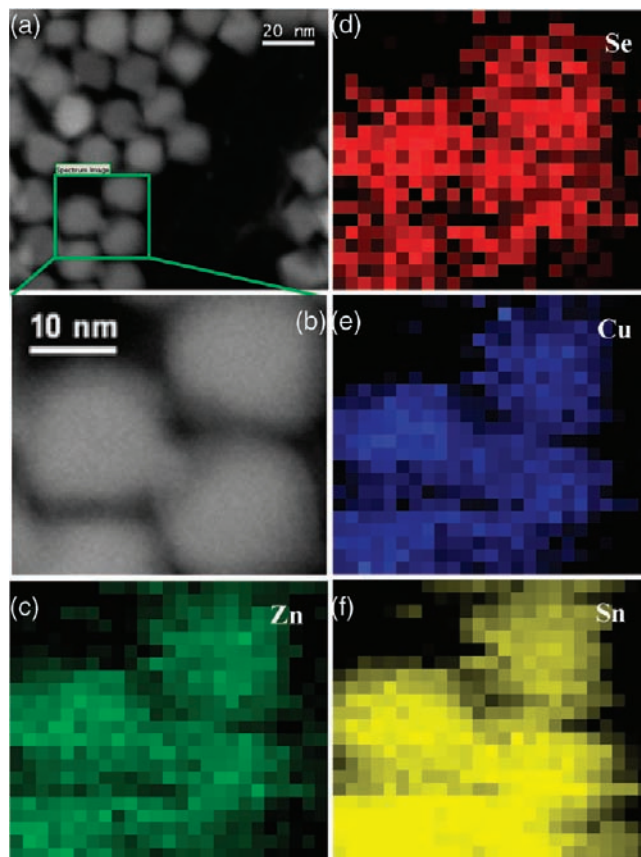


Figure 4. (a, b) Z-contrast STEM images of the CZTSe nanoparticles. (c–f) EELS elemental mapping images: (c) Zn; (d) Se; (e) Cu; (f) Sn.

Acknowledgment. This work was supported by the Spanish MICINN Projects MAT2008-05779 and ENE2008-03277-E/CON. J.A. is an ICREA Research Professor.

Supporting Information Available: Detailed experimental procedure; additional Z-contrast STEM, EELS, EDX, and XPS analysis data; the CZTSe unit cell; and a 3D atomic model of a 10 nm diameter CZTSe nanoparticle. This material is available free of charge via the Internet at <http://pubs.acs.org>.

References

- (1) Riha, S. C.; Parkinson, B. A.; Prieto, A. L. *J. Am. Chem. Soc.* **2009**, *131*, 12054.
- (2) Guo, Q.; Hillhouse, H. W.; Agrawal, R. *J. Am. Chem. Soc.* **2009**, *131*, 11672.
- (3) Steinhagen, C.; Panthani, M. G.; Akhavan, V.; Goodfellow, B.; Koo, B.; Korgel, B. A. *J. Am. Chem. Soc.* **2009**, *131*, 12554.
- (4) (a) Chen, S.; Gong, X. G.; Walsh, A.; Wei, S. *Appl. Phys. Lett.* **2009**, *94*, 041903. (b) Grossberg, M.; Krustok, J.; Timmo, K.; Altsaar, M. *Thin Solid Films* **2009**, *517*, 2489. (c) Liu, M.; Chen, I.; Huang, F.; Chen, L. *Adv. Mater.* **2009**, *21*, 3808. (d) See the Supporting Information for details.
- (5) Babu, G. S.; Kumar, Y. B. K.; Bhaskar, P. U.; Raja, V. S. *J. Phys. D: Appl. Phys.* **2008**, *41*, 205305.
- (6) Liu, M. L.; Huang, F. Q.; Chen, L. D.; Chen, I. W. *Appl. Phys. Lett.* **2009**, *94*, 202103.
- (7) Wibowo, R.; Kim, W.; Lee, E.; Munir, B.; Kim, K. *J. Phys. Chem. Solids* **2007**, *68*, 1908.
- (8) Wibowo, R.; Lee, E.; Munir, B.; Kim, K. *Phys. Status Solidi A* **2007**, *204*, 3373.
- (9) Olekseyuk, I.; Gulay, L.; Dydchak, I.; Piskach, L.; Parasyuk, O.; Marchuk, O. *J. Alloys Compd.* **2002**, *340*, 141.
- (10) Shi, X. Y.; Huang, F. Q.; Liu, M. L.; Chen, L. D. *Appl. Phys. Lett.* **2009**, *94*, 122103.
- (11) Chen, S.; Gong, X.; Walsh, A.; Wei, S. *Phys. Rev. B* **2009**, *79*, 165211.

JA909498C